Path Synthesis of Planar Linkage Mechanisms Using Deep Generative Models

Abhay Bhaskar
Dept. of Mechanical Engineering
Stony Brook University
Stony Brook, United States
abhaybhaskar2603@gmail.com

Anar Nurizada
Dept. of Mechanical Engineering
Stony Brook University
Stony Brook, United States
anar.nurizada@stonybrook.edu

Anurag Purwar
Dept. of Mechanical Engineering
Stony Brook University
Stony Brook, United States
anurag.purwar@stonybrook.edu

***Abstract*—The problem of path generation of planar mechanisms, or determining their motion as traced by a coupler curve, has been almost exclusively met with analytical solutions, leading to high run-time and low efficiency. In contrast, our approach utilizes a Machine Learning model, implementing a novel approach combining a generative AI model known as a Variational Autoencoder with a Fully Connected Neural Network to produce four-bar, six-bar, and eight-bar mechanisms to fit a desired path. We also determine which representations of the input coupler curve lead to the most accurate mechanisms. This work significantly improves the efficiency and automation of mechanism design.**

***Keywords*—Planar four-, six-, and eight-bar linkage systems, path synthesis, Fourier descriptors, Wavelets, Variational Autoencoder, Neural Networks, Machine Learning**

I. Introduction

The problem of path synthesis of planar mechanisms, or determining the parameters of a mechanism such that its motion follows a sequence of consecutive points (x_i,y_i) in R^2, has been extensively studied and had a plethora of proposed solutions. Most of the prior solutions have used an analytical approach to find the path of a mechanism's motion, traced by a **coupler curve**. However, this has led to problems such as high run-time and a necessity for greater computational resources. To combat this, in recent years, Neural Networks have been proposed as a potential tool for the design of these mechanisms, called kinematic synthesis. This is mainly due to their ability to learn a mapping from the design specifications of a mechanism to its dimensional parameters.

The main issue with the application of Neural Networks to this problem is the representation of mechanisms and their properties, which form a non-Euclidean space. To resolve this, a Euclidean embedding is used on the input path, resulting in different representations of the input coupler curves of the mechanism: Fourier Descriptors, Wavelet Descriptors, (x,y) points on the curve, and Images. These representations have on occasion been explored and had their effectiveness compared for various tasks. Osowski and Nghia [1] compared the use of Fourier Descriptors and Wavelet Descriptors for feature extraction in 2D space. They found that Wavelet Descriptors yielded a much higher accuracy. Li et al. [2] conducted a study to compare these two input representations in flaw classification and came to the same conclusion. Deshpande and Purwar [3] trained a Convolutional Neural Network on images of coupler curves to synthesize four-bar and six-bar linkage systems that closely fit an input path. However, there has been no comparative study on a single dataset to examine the accuracy of all four of these input representations in the generation of mechanisms to achieve a desired motion. This has proven to be a major obstacle to Machine Learning applications in kinematic synthesis, as identifying which feature, or representation, would be best to extract from a coupler curve is key for the training of these models.

In addition to providing a measure of the effectiveness of each input representation, this paper presents a Machine Learning approach for the synthesis of four-bar, six-bar, and eight-bar linkage systems that approximate a desired coupler curve. The model consists of a Variational Autoencoder (VAE) and a Fully Connected Neural Network (FCNN) to generate many possible linkage systems to closely match the input motion. It was tested on the four input representations mentioned: Fourier Descriptors, Wavelet Descriptors, (x,y) points on the curve, and Images. The full pipeline is depicted visually in Fig. 1.

Through the use of Machine Learning, this paper makes great improvements in how mechanisms are designed, efficiently providing a wide variety of linkage systems to approximate a certain motion. This could be utilized in many different fields, including robotics, prosthetics, and other assistive-technologies. It also identifies which input representations are best to represent the coupler curves of various mechanisms, an important question that has not been previously answered.

II. Input Representations

In this project, four different input representations of a coupler curve were used to assess which led to the model producing the most accurate mechanisms: Fourier Descriptors, Wavelet Descriptors, (x,y) points on the curve, and Images.

Fourier Descriptors transform 2D (x, y) points to 1D and describe closed curves. They are expressed by:

$$a_m = \sum_{k=0}^{N-1} z_k e^{2\pi mk/N} \tag{1}$$

where $z = x+iy$, N is the total number of points, and a_m is the Fourier Descriptor. McGarva and Mullineux [4] first used

979-8-3503-0965-2/23/$31.00

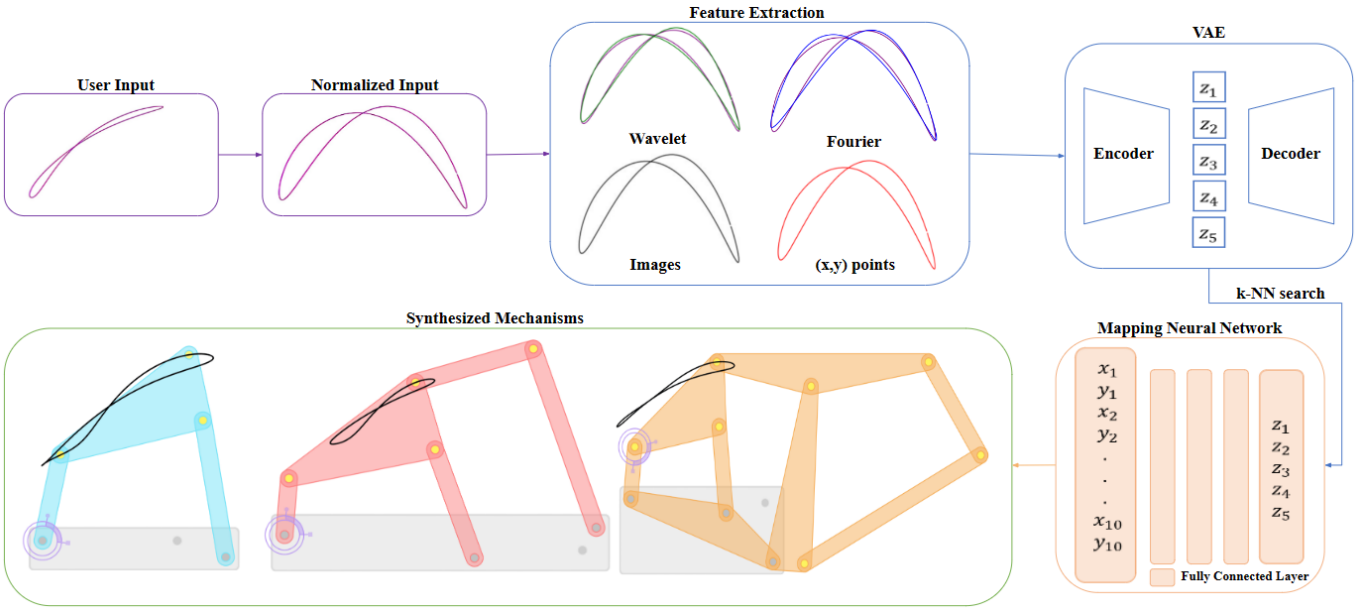

Fig. 1: Full pipeline created in this paper. The curves were first normalized so they were invariant with respect to dilation, translation, and rotation. Next, each of the four input representations were extracted and fed into their respective pre-trained VAEs, which mapped the curve to a latent space. From here, a k-Nearest Neighbors (k-NN) search was used to find 10 similar coupler curves represented as latent vectors that then served as the input to the FCNN. This output 10 generated mechanisms that approximated the input coupler curve.

them for curve representation, finding the fundamental (a_0) and first harmonic terms (a_1 and a_{-1}) particularly useful. Li et al. [5] found that $m = 5$ is sufficient for the coupler curves of four-bar linkage systems. In this paper, a second case was checked where $m = 10$ to determine if increasing the number of harmonics yielded a significant difference in the quality of the mechanisms generated, and if $m = 5$ was also viable for six-bar and eight-bar mechanisms.

Wavelet Descriptors are mathematical functions used in signal processing to represent data at various resolutions. The most commonly used wavelet is the Daubechies Wavelet, defined by:

$$\psi_{a,b}(x) = \frac{1}{\sqrt{a}} \sum_{k=-\infty}^{\infty} h(n) e^{2\pi i \frac{nx-b}{a}} \tag{2}$$

where $h(n)$ represents the wavelet descriptor, a is the scaling factor, and b is the translation factor. Wavelet descriptors can be derived from scaling function descriptors, using the following formula:

$$h(n) = (-1)^n \sum_{k=0}^{n} (-1)^k \binom{n}{k} f(k) \tag{3}$$

in which $f(k)$ denotes the sequence of scaling function descriptors, and n is the index of the wavelet descriptor.

Chuang and Kuo [6] used Wavelet Descriptors to represent closed planar curves, studying both general and detailed aspects of the curve. Wavelet descriptors are often obtained using a wavelet transform, breaking down a signal into different components by frequency. In this paper, the x and y-coordinates of points on the coupler curves were treated as separate signals, and a five-level decomposition with Daubechies wavelets was performed with two quantities of descriptors: 44 and 76. We determined that 44 wavelet descriptors was sufficient to approximate a coupler curve, and a higher value was also checked to gauge the impact of varying the number of descriptors on the accuracy of the output mechanisms.

(x,y) points and Images are much more self explanatory. For the former, a sequence of (x,y) points on the coupler curve was chosen as the input. There were two different cases using this input representation, one with 180 (x,y) points, and another with 360 (x,y) points, allowing for analysis of the trade-off in the input quantity vs the accuracy of the resulting mechanisms. 64×64 pixels images of the coupler curves were used as the fourth and final representation.

III. Dataset Creation and Normalization

As with many Machine Learning models, one issue that arose was the lack of publicly accessible datasets that could be used. Nobari et al. [7] created LINKS, a dataset of one hundred million planar mechanisms, for use in kinematic design. However, such a dataset was too expansive for our purposes, as it contains mechanisms much larger than eight-bar linkage systems and would require significant computation time and resources.

As such, an algorithm was created to find valid four-bar, six-bar, and eight-bar linkage systems, with the goal of filling the dataset with mechanisms that satisfied the Grashof Condition. First, a 17×17 grid of points was created, ranging from -2 to

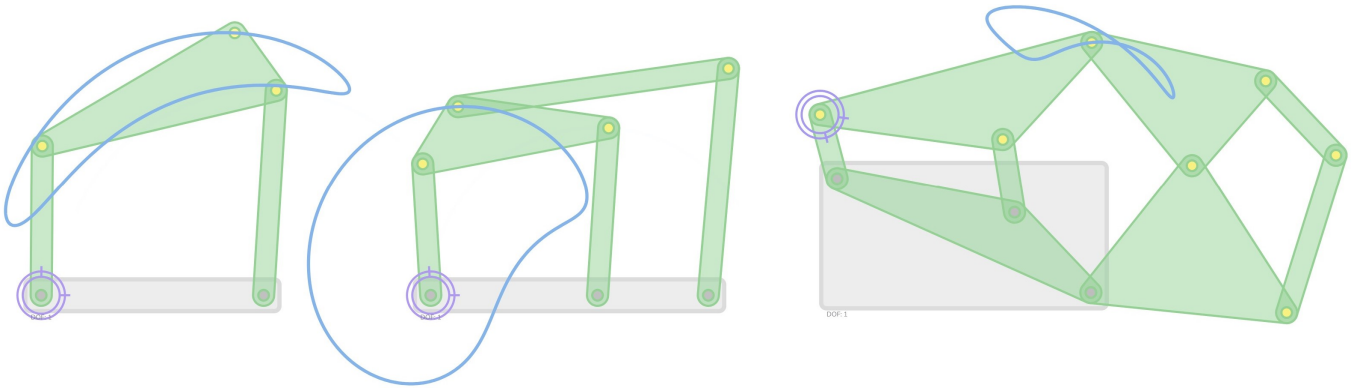

Fig. 2: Left to right: Four-Bar, Six-Bar (Stephenson III), and Eight-Bar Linkage System Topologies.

2, inclusive, with increments of 0.25 in the (x, y) plane. From there, various combinations of points were selected to serve as the joints' locations of the mechanisms, with the number selected depending on the type of linkage system. Our goal was to create a dataset of mechanisms with a diverse set of coupler curves. These curves had to be closed so that Fourier Descriptors and Wavelet Descriptors could be extracted from them.

For the **four-bar** linkage systems, mechanisms were generated using sets of five points randomly selected from the grid. These points represented the locations of the fixed and moving joints of mechanisms, which were then added to the dataset only if their link ratios ($\frac{l_1}{l_0}, \frac{l_2}{l_0}, \frac{l_3}{l_0}$) were distinct, where l_0, l_1, l_2, and l_3 denote the ground, input, output, and coupler links, respectively. Moreover, mechanisms failing to satisfy the Grashof condition, leading to open coupler curves, were not included in the dataset.

The **six-bar** linkage mechanisms were generated using sets of seven points from the grid. The topology selection was focused on Stephenson III. Additionally, the computed coupler curves were verified to be closed. Using combinations of ten points from the grid, the **eight-bar** linkage systems were generated. Similar to the previous cases, only mechanisms resulting in the closed coupler curves were added to the dataset.

The complete dataset comprised 9000 mechanisms divided equally among the three linkage systems, all of which exclusively produced closed coupler curves. Sample mechanisms from each topology are displayed in Fig. 2.

In this study, each coupler curve underwent a **normalization procedure** to ensure translation, scale, and rotation invariance. The normalization involved centering the curve around $(0, 0)$ by subtracting the mean $(\bar{x}, \bar{y})$ from each coupler point (x_i, y_i). Scaling was then applied by dividing the points by the root mean squared variance in both x- and y-directions. The orientation was normalized by finding the principal component axes, achieved through eigenvectors of the covariance matrix C. A rotation technique aligned the principal component axes with the Cartesian coordinate system, standardizing the curve's orientation. It is important to note that mirrored mechanisms and their coupler curves were not normalized, treated as distinct entities, and mapped to separate locations in the latent space.

IV. The Machine Learning Model and k-Nearest Neighbors (k-NN) Search

The entire model was broken down into two parts, a Variational Autoencoder and a Fully Connected Neural Network. The **Variational Autoencoder (VAE)** consisted of two parts, an encoding model and a decoding model. The encoding model took in an input representation of the coupler curve and mapped it to a 5D latent space, compressing it to a 5×1 column vector. After this, the decoding model took the latent vector and attempted to reconstruct the input coupler curve. The VAE was trained to become more accurate, and this accuracy was measured by a two-part loss function:

$$\mathcal{L}_{\text{VAE}} = \mathbb{E}_{q(z|x)} \left[\log p(x \mid z)\right] - \text{KL}\left(q(z \mid x) \| p(z)\right) \tag{4}$$

In this equation, x denotes the input while z is the latent vector. This loss is composed of two parts. The first is the reconstruction loss, or the difference between the input and its reconstruction. The second component is the Kullback-Leibler Divergence, or how much the distribution of the latent space differs from a Gaussian Distribution, with a mean of 0 and standard deviation of 1. The Variational Autoencoder was trained for 200 epochs, where each epoch looked through all of the coupler curves in the dataset exactly once. The architecture of the VAE is shown in Table I, with a variable q for the initial input neuron and final output neuron since this value will vary depending on the input representation. The ReLU activation function was used.

The **Fully Connected Neural Network (FCNN)** was the second part of the pipeline, which used fully connected layers with the ReLU activation function. The architecture is shown in Table II. The FCNN took the latent vector of the coupler curve from the pre-trained VAE as its input, outputting the x and y coordinates of the joint locations. The loss used to train the FCNN was the Mean Squared Error (MSE) between the input and predicted joint locations. As with the VAE, the FCNN was trained for 200 epochs, and the ReLU activation function was used.

TABLE I: VAE Architecture

Layer/Activation Function	Input Neurons	Output Neurons
Encoder		
Dense (ReLU)	q	120
Dense (ReLU)	120	120
Dense (ReLU)	120	120
Dense (ReLU)	120	120
Dense (ReLU)	120	120
Dense (ReLU)	120	120
Dense (ReLU)	120	120
Latent Space: Mean	120	5
Latent Space: Variance	120	5
Decoder		
Dense (ReLU)	5	120
Dense (ReLU)	120	120
Dense (ReLU)	120	120
Dense (ReLU)	120	120
Dense (ReLU)	120	120
Dense (ReLU)	120	120
Dense (-)	120	q

TABLE II: Fully Connected Neural Network Architecture

Layer/Activation Function	Input Neurons	Output Neurons
Dense (ReLU)	5	1280
Dense (ReLU)	1280	1280
Dense (ReLU)	1280	1280
Dense (ReLU)	1280	1280
Dense (ReLU)	1280	1280
Dense (ReLU)	1280	1280
Dense (ReLU)	1280	1280
Dense (ReLU)	1280	1280
Dense (ReLU)	1280	20

The output was a 20×1 column vector, with the first 10 neurons corresponding to the 5 joint locations (x and y-coordinates) of a four-bar linkage system, the next 4 neurons corresponding to the additional 2 joints present in a six-bar linkage system, and the final 6 neurons capturing the additional 3 joints present in an eight-bar linkage system. To figure out whether the output mechanism was a four-bar, six-bar, or eight-bar, the neurons were closely examined. If the output was a four-bar linkage system, then the output of the last ten neurons were all close to 0 (within 0.01). If the output was a six-bar linkage system, then the output of the last six neurons would be close to 0. Otherwise, the output mechanism was determined to be an eight-bar linkage system. It should be noted that even after the training process, the FCNN did not predict these empty joint locations to be exactly 0, meaning that a small range had to be allowed for.

To obtain multiple mechanisms, two methods were employed. First, a **k-Nearest Neighbors (k-NN) Search** was conducted using the input coupler curve's latent vector from the pre-trained VAE. The ten nearest coupler curves, represented as latent points, were found in the dataset's latent space. These latent vectors were then fed into a FCNN to generate joint locations and synthesize the output mechanisms along with their coupler curves.

The second method involved sampling new latent codes in the vicinity of the input coupler curve's latent representation. The Euclidean distance between the sampled and input latent vectors determined the similarity. A distance of 0.01 mostly yielded mechanisms of the same type as the input, while greater distances led to a wider variety of four-, six-, and eight-bar linkage systems being generated. Notably, a distance of 0.05 and higher resulted in significantly different coupler curves for the generated mechanisms when compared to that of the input mechanism.

TABLE III: Results for Input Representations

Input Representation	MSE Loss	k-MSE Loss
22 Fourier Descriptors	0.227	1.037
42 Fourier Descriptors	0.236	0.919
44 Wavelet Descriptors	0.311	0.473
76 Wavelet Descriptors	0.268	0.419
180 (x,y) Points	0.258	0.409
360 (x,y) Points	0.246	0.354
Images	0.59	1.87

V. Results

Examples of the synthesized mechanisms output by this pipeline are shown in Fig. 3 and 4. In Fig. 3, three four-bar linkage systems were synthesized to fit an input coupler curve. Out of all types of mechanisms, four-bars are the most widely used. As a result, it was important to examine multiple synthesized four-bar linkage systems. Six-bar and eight-bar linkage systems are also utilized in many fields, making it critical to test their accuracy as well. This meant that the model also needed to be able to synthesize six-bar and eight-bar mechanisms to closely fit the input path, as displayed in Fig. 4.

To assess the accuracy of different representations and the overall pipeline, various metrics were employed to quantify the outcomes. The initial measurement involved the use of Mean Squared Error (MSE) to calculate the disparity between the desired (input) curve and its optimal approximation. It's worth noting that a well-trained pipeline would necessitate the predicted joints to align with the true joints, thus establishing a one-to-one correspondence between the points on both curves. Without this, it would not have been possible to properly evaluate the model's accuracy.

A secondary assessment was conducted to gauge how multiple mechanisms could fit a certain motion. This involved predicting ten different mechanisms to approximate a single input coupler curve, and then averaging the MSE losses across all mechanisms, denoted as the k-MSE loss. The outcomes of both these evaluations are detailed in Table III.

An analysis of the loss values revealed which input representations produce the most favorable results. The use of (x, y) points as the input was found to lead to the most accurate generation of k mechanisms, closely followed by Wavelet Descriptors. Though Fourier Descriptors and Images were somewhat less effective, all four representations yielded mechanisms that provided a reasonable approximation of the coupler curve, with similar outcomes. Moreover, augmenting the number of descriptors or points did enhance the accuracy

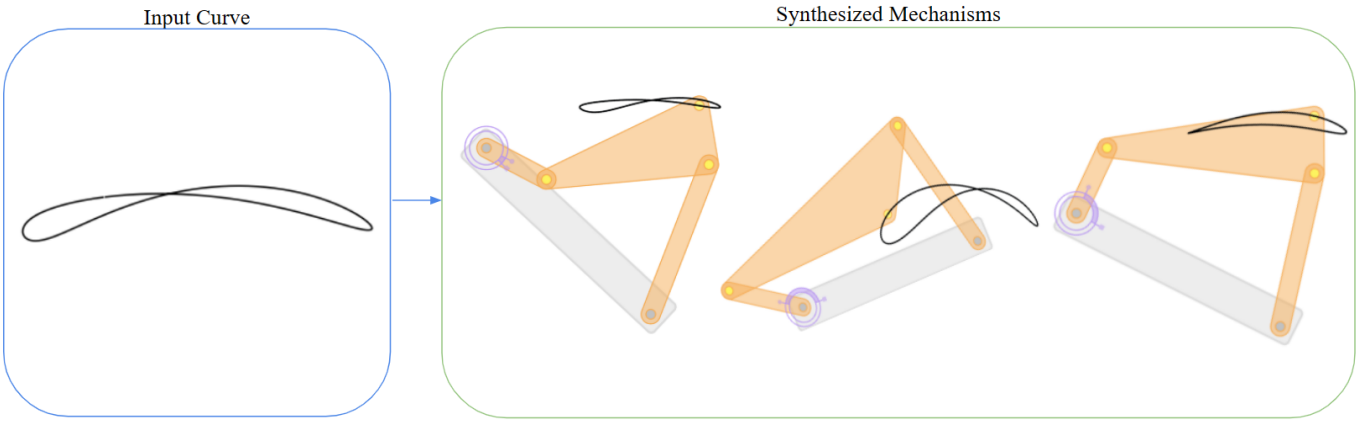

Fig. 3: Four-Bar Linkage Systems Synthesized from an Input Coupler Curve

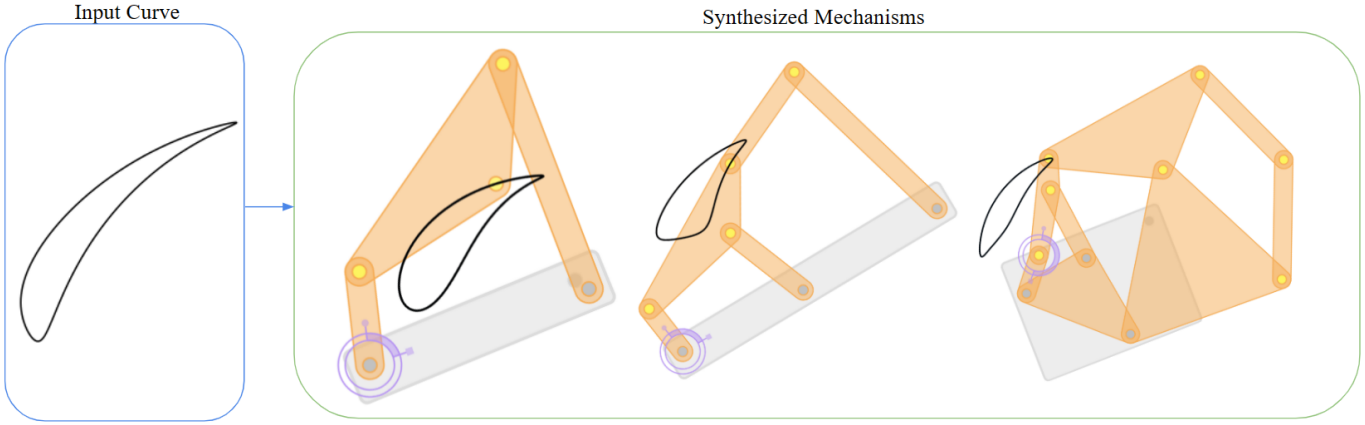

Fig. 4: Four-Bar, Six-Bar, and Eight-bar Linkage Systems Synthesized from an Input Coupler Curve

of the generated mechanisms; however, the practicality of this approach will vary, depending on multiple context-specific factors.

Conclusion

This paper presents a novel approach using Machine Learning to produce accurate four-, six-, and eight-bar linkage systems to fit the motion of an input mechanism. The pipeline's accuracy in generating mechanisms using the latent representation of coupler curves through the VAE demonstrates its ability to serve as an independent representation, regardless of the extracted feature. The study also identifies (x, y) points and Wavelet Descriptors as the most accurate input representations, but all four options perform well. Additionally, understanding how increasing descriptors or points affects the quality of synthesized mechanisms offers flexibility for practical applications in various industries. This information is valuable for researchers utilizing Machine Learning for mechanism design, seeking a faster and more efficient alternative to the current analytical approaches. Overall, the promising results of this project make great strides in the automation of mechanism design.

References

[1] Osowski, S. and Nghia, D. D., 2002, "Fourier and wavelet descriptors for shape recognition using neural networks–a comparative study", Pattern Recognition, **35(9)**, pp. 1949–1957–1949–1957, doi:10.1016/s0031-3203(01)00153-4.

[2] Li, L., Cheng, W., Tsukada, K., and Hanasaki, K., 2004, "Flaw Classification by Using Artificial Neural Network and Wavelet", ASMEDC, doi:10.1115/pvp2004-2815.

[3] Deshpande, S. and Purwar, A., 2020, "An Image-Based Approach to Variational Path Synthesis of Linkages", ASME Journal of Computing and Information Science in Engineering, **21(2)**, doi:10.1115/1.4048422, URL https://doi.org/10.1115/1.4048422, 021005.

[4] Mcgarva, J. and Mullineux, G., 1993, "Harmonic Representation of Closed Curves", Applied Mathematical Modelling, **17(4)**, pp. 213–218.

[5] Li, X., Wu, J., and Ge, Q. J., 2016, "A Fourier Descriptor-Based Approach to Design Space Decomposition for Planar Motion Approximation", ASME Journal of Mechanisms and Robotics, **8(6)**, pp. 064501–064501–5, 10.1115/1.4033528.

[6] Chuang, G. C.-H. and Kuo, C.-C. J., 1996, "Wavelet descriptor of planar curves: theory and applications", IEEE Transactions on Image Processing, **5(1)**, pp. 56–70–56–70, doi:10.1109/83.481671.

[7] Nobari, A. H., Srivastava, A., Gutfreund, D., and Ahmed, F., 2022, "LINKS: A Dataset of a Hundred Million Planar Linkage Mechanisms for Data-Driven Kinematic Design", Volume 3A: 48th Design Automation Conference (DAC), American Society of Mechanical Engineers, doi:10.1115/detc2022-89798.